ARTICLE

Check for updates

Clinical profiling of MRD48 and functional characterization of two novel pathogenic *RAC1* variants

Manuela Priolo[1,9✉], Erika Zara[2,3,9], Francesca Clementina Radio[2], Andrea Ciolfi[2], Francesca Spadaro[4], Emanuele Bellacchio[2], Cecilia Mancini[2], Francesca Pantaleoni[2], Viviana Cordeddu[5], Luigi Chiriatti[1], Marcello Niceta[2], Emilio Africa[6], Corrado Mammì[1], Daniela Melis[7], Simona Coppola[8] and Marco Tartaglia[2✉]

© The Author(s), under exclusive licence to European Society of Human Genetics 2023

RAC1 is a member of the Rac/Rho GTPase subfamily within the RAS superfamily of small GTP-binding proteins, comprising 3 paralogs playing a critical role in actin cytoskeleton remodeling, cell migration, proliferation and differentiation. De novo missense variants in *RAC1* are associated with a rare neurodevelopmental disorder (MRD48) characterized by DD/ID and brain abnormalities coupled with a wide range of additional features. Structural and functional studies have documented either a dominant negative or constitutively active behavior for a subset of mutations. Here, we describe two individuals with previously unreported de novo missense *RAC1* variants. We functionally demonstrate their pathogenicity proving a gain-of-function (GoF) effect for both. By reviewing the clinical features of these two individuals and the previously published MRD48 subjects, we further delineate the clinical profile of the disorder, confirming its phenotypic variability. Moreover, we compare the main features of MRD48 with the neurodevelopmental disease caused by GoF variants in the paralog *RAC3*, highlighting similarities and differences. Finally, we review all previously reported variants in RAC proteins and in the closely related CDC42, providing an updated overview of the spectrum and hotspots of pathogenic variants affecting these functionally related GTPases.

European Journal of Human Genetics (2023) 31:805–814; https://doi.org/10.1038/s41431-023-01351-7

INTRODUCTION

Rho GTPases are small proteins belonging to the RAS superfamily functioning as signal transducers in pathways that control cell proliferation, differentiation and survival, being key regulators of actin polymerization [1]. The Rho GTPases family can be divided into eight subgroups comprising at least 22 members [2]. They are molecular switches cycling between active (GTP-bound) and inactive (GDP-bound) states through conformational changes in their Switch I and Switch II regions, and are characterized by a *C*-terminal CAAX motif, which undergoes post-translational modifications [2, 3]. Dysfunction of Rho GTPases and their regulators is a key event in various pathological processes, including oncogenesis and clinical evolution of adult-onset neurodegenerative diseases [4, 5].

Among Rho GTPases, the RAS-related C3 Botulinum toxin substrate (RAC) subfamily comprises 3 proteins (RAC1 to 3), which share about 90% of homology in their amino acid sequence [6]. *RAC1* (MIM 602048) is one of the major regulators of actin cytoskeleton remodeling, controlling cell migration, axon outgrowth, dendritic arborization, and synaptogenesis [7, 8]. *RAC1* is ubiquitously expressed [9]; differently, *RAC2* (MIM 602049) is almost confined to hematopoietic cells, and *RAC3* (MIM 602050) is specifically expressed in both developing and adult nervous system [10, 11].

Germline mutations affecting members of the RAC family have been causally linked to clinically heterogeneous developmental disorders [3, 7, 12, 13]. Heterozygous and biallelic pathogenic *RAC2* variants cause primary immunodeficiency with variable presentation, ranging from granulocytes defects to combined immunodeficiency (MIM 618987, 608203 and 618986) [13]. *RAC3* is mutated in an autosomal dominant neurodevelopmental disease (NDD) characterized by structural brain anomalies and facial dysmorphisms (NEDBAF; MIM 618577) [12]. Similarly, mutations in *RAC1* underlie an autosomal dominant NDD characterized by a wide spectrum of clinical features, including facial dysmorphisms and intellectual disability (ID) (MRD48; MIM 617751) [7, 14, 15]. To date, missense variants affecting seven conserved residues located throughout the protein have been observed in eight unrelated individuals. In vitro functional characterization of a subset of variants demonstrated opposite effects on cell morphology, with two mutants (i.e., C18Y and N39S) having a dominant negative (DN) behavior, and one (i.e., Y64D) working as a constitutively active (CA) protein, with mirroring effects on filopodia/lamellipodia/ruffle protrusions and cellular roundness index (RI) [7]. The remaining mutants could not be clearly classified in the same experimental model although exhibiting some functional intermediate effect on both cellular morphology

[1]USD Genetica Medica, Grande Ospedale Metropolitano Bianchi-Melacrino-Morelli, 89124 Reggio Calabria, Italy. [2]Molecular Genetics and Functional Genomics, Ospedale Pediatrico Bambino Gesù, IRCCS, 00146 Rome, Italy. [3]Department of Biology and Biotechnology, Sapienza University, 00185 Rome, Italy. [4]Core Facilities, Istituto Superiore di Sanità, 00161 Rome, Italy. [5]Department of Oncology and Molecular Medicine, Istituto Superiore di Sanità, 00161 Rome, Italy. [6]USD Neuroradiologia, Grande Ospedale Metropolitano Bianchi-Melacrino-Morelli, 89124 Reggio Calabria, Italy. [7]Department of Medicine, Surgery and Dentistry "Scuola Medica Salernitana", Università di Salerno, 84084 Salerno, Italy. [8]National Center for Rare Diseases, Istituto Superiore di Sanità, 00161 Rome, Italy. [9]These authors contributed equally: Manuela Priolo, Erika Zara.
✉email: prioloma@libero.it; marco.tartaglia@opbg.net

Received: 21 November 2022 Revised: 10 March 2023 Accepted: 21 March 2023
Published online: 14 April 2023

and RI. Among the studied variants, the C18Y substitution was also documented to prevent GTP-mediated RAC1 activation, with an increased dendritic spine density eventually precluding synaptic transmission [16].

Mirroring the molecular complexity of *RAC1* mutations, affected individuals show a noteworthy phenotypic variability with different degrees of DD/ID, neurological abnormalities, and facial dysmorphisms [7, 15]. The most remarkable clinical finding is the stark variability in the occipital-frontal circumference (OFC), ranging from −5.0 to +4.5 SD, with a few subjects showing normal values (Table 1). This heterogeneity correlates with specific mutations, as the DN mutants (C18Y and N39S), which were reported in subjects with microcephaly, have also been demonstrated to induce a significant decrease in head size in zebrafish embryos [7].

Here, we describe two additional individuals with previously unreported de novo missense variants in *RAC1* and a NDD characterized by normal OFC, facial dysmorphisms, mild/moderate DD/ID and a variable range of additional signs, confirming the clinical variability of MRD48. For both variants, we demonstrate their gain-of-function (GoF) impact. We clinically review the disorder and deeply delineate the common clinical and facial features. We also compare the main clinical presentations of MRD48 and NEDBAF, highlighting similarities and differences. Finally, we revise the mutation spectrum in RAC1-3 and CDC42, the latter being an additional Rho GTPase sharing considerable homology with RAC proteins previously associated with a highly heterogeneous phenotypic presentation [17, 18], evidencing the occurrence of a recurring pattern of mutational hotspots.

MATERIALS AND METHODS

Subjects and molecular analysis

Both subjects were enrolled in the context of a research program aimed at understanding the molecular causes of unclassified pediatric disorders at the Ospedale Pediatrico Bambino Gesù, Rome, Italy. The study has been approved by the local Institutional Ethical Committee (ref. 1702_OPBG_2018). Clinical data, pictures, DNA samples and other biological specimens were collected, used, and stored after signed informed consents from the participating subjects/families were secured. Permission to publish the clinical pictures was obtained for both individuals.

A trio-based whole-exome sequencing (WES) was performed on both subjects after the exclusion of any clinically relevant structural variant by high-resolution CMA analysis. Genomic DNA of the affected subjects and their parents was extracted from leukocytes and sequenced using Illumina paired-end technology coupled with the SureSelect AllExon V.7 (Aligent Technologies, Santa Clara, CA) enrichment kit. Sequencing protocol, WES statistics, reads alignment and variant calling pipelines, data processing and output are detailed in Supplementary Materials and Methods and reported in Table S1. Selected variants were validated *via* Sanger sequencing following standard protocols. The identified pathogenic *RAC1* variants have been submitted to ClinVar (SCV002605544, SCV002605545).

Structural analysis

The crystal structure of RAC1 in complex with the KALRN DH1 domain (PDB accession: 5O33) was employed to display the sites affected by the identified amino acid substitutions. Molecular graphs were made with PyMOL (www.pymol.org).

Cell lines and cultures

HEK-293T and COS-1 cell lines were obtained from American Type Culture Collection (ATCC) and grown in high-glucose Dulbecco's modified Eagle's medium (DMEM) supplemented with 10% fetal calf serum, 2 mM L-glutamine, 10 U/ml penicillin/streptomycin, and 1 mM sodium pyruvate (Merck, Darmstadt, Germany).

RAC1 levels and GTP binding assay

Wild-type human *RAC1* (NM_006908.4) was cloned into a pcDNA3 backbone with an *N*-terminal HA tag. Mutant constructs expressing the E62K, A159T, A159V or G12V amino acid substitutions were generated by site-directed mutagenesis using the QuikChange XL kit (Agilent Technologies), and verified by direct sequencing. Each of the HA-tagged *RAC1* constructs or the empty vector was transfected using Fugene 6 (Roche, Basel, Switzerland). Two days after transfection, cells were assayed for RAC1 levels, GTP-bound state and function, which were verified by western blot and pull-down assays (see Supplementary Materials and Methods) or processed for immunofluorescence analysis. For protein stability studies, cells were treated up to 6 h with MG132 (50 μM) and then lysed for RAC1 levels assays.

Cell shape assay by immunofluorescence and confocal microscopy analysis

Immunofluorescence analyses were performed as previously described [19]. Complete protocol is detailed in Supplementary Materials and Methods. Confocal laser scanning microscopy observations were performed with a LSM980 apparatus (Zeiss, Oberkochen, Germany), using a 63x/1.40 NA oil objective and excitation spectral laser lines at 405, 488, 594 nm. Cell roundness was calculated by using the formula roundness index $= \frac{perimeter}{2\sqrt{\pi\ area}}$, as previously reported [20]. The mean perimeter and area of cells were calculated using the Image J software [21], drawing the region of interest based on f-actin fluorescence delimited borders. At least 20 cells were analyzed for each dataset. Data were pooled from three independent experiments and highly expressing cells were excluded.

Statistical analysis

Data were represented as means ± SEM. Statistical analyses were performed using GraphPad Prism version 5.0. (GraphPad Software, San Diego, CA). GTPase function and RI measurements were analyzed by multiple *t*-test, corrected for multiple comparisons using Holm-Sidak method and Chi-square's test in 2 × 2 contingency tables (Fisher's exact test), respectively. Statistical significance is indicated with asterisks: $*p < 0.05$, $***p < 0.001$, $****p < 0.0001$. Comparisons of clinical features were calculated by using the Fisher's exact test.

RESULTS

Genomic analyses

Molecular analyses identified two de novo missense variants, c.475G>A (p.Ala159Thr [A159T], subject 1) and c.184G>A (p.Glu62Lys [E62K], subject 2) within exons 7 and 3 of *RAC1* (NM_006908.5, NP_008839.2). Sanger sequencing of probands' DNA specimens collected from additional tissues proved both variants to be germline. The two variants had not previously been reported in neither public (e.g., gnomAD v.2.1.1) nor in-house (>2800 exomes) population databases, and were classified as pathogenic according to the ACMG/AMP criteria [22] (Supplementary Table S2). All tested in silico pathogenicity scores pointed out these changes as disease-causing. Consistently, a strong evolutionary constraint for the affected amino acids was evidenced, further supporting a deleterious effect (90% classification accuracy) of the reported changes [23].

In Subject 2, the segregation from an affected father of hearing impairment suggested a possible double diagnosis to be investigated. Filtering for private or low-frequency variants in genes associated with deafness allowed to identify a nonsense variant in *GRHL2* (c.108G>A, p.Trp36*; NM_024915.4), which was classified as pathogenic according to the ACMG guidelines. Loss-of-function (LoF) variants in *GRHL2* are associated with a form of late-onset autosomal dominant non-syndromic hearing loss (DFNA28; MIM 608641).

Functional characterization of the E62K and A159T substitutions

To investigate the effects of E62K and A159T amino acid changes on RAC1 function, we analyzed protein levels in lysates of COS-1 cells transiently transfected with HA-tagged *RAC1* wild-type (WT), each of the two mutants, and RAC1 proteins carrying the A159V (oncogenic) or G12V (CA) variants [24, 25]. Western blot analysis documented similar levels of $RAC1^{A159T}$ with respect to the WT

Table 1. Clinical and molecular data of report individuals and present cases.

	Present report		[7]							[15]	*Total*
Subjects	1	2	A	B	C	D	E	F	G	K	*N* = 10
Sex (age)	M	F	M	M	M	M	M	M	M	F	8M/ 2F/
cDNA change	c.475G>A	c.184G>A	c.53G>A	c.116A>G	c.218C>T	c.470G>A	c.190T>G	c.151G>A	c.151G>C	c.94T>C	
aa change	p.A159T	p.E62K	p.C18yr	p.N39S	p.P73L	p.C157Y	p.Y64D	p.V51M	p.V51L	p.Y32H	
GROWTH AND FACIAL DYSMORPHISMS											
Height	131.5 cm (−1.23 SD)	160 cm (−0.5 SD)	127 cm (−2.5 SD)	128 cm (−2.5 SD)	n.r.	62 cm (−1 SD)	134 cm (+1.03 SD)	n.r.	109 cm (0 SD)	n.r.	
Weight	27 kg (−1.16 SD)	56 kg (−0.19 SD)	30 kg (0 SD)	24 kg (−0.5 SD)	n.r.	4.8 kg (−3 SD)	n.r.	n.r.	23 kg (+2.5 SD)	n.r.	
Head circumference	52.7 cm (−0.64 SD)	55 cm (+0.63 SD)	50 cm (−2.5 SD)	47.7 cm (-3 SD)	47 cm (−5 SD)	39 cm (−2.5 SD)	56.5 cm (+1 SD)	57 cm (+4.16 SD)	59.5 cm (+4.5 SD)	n.r.	
Facial dysmorphisms[a]	Yes	Yes	Yes	Yes	Yes	Yes	Yes	Yes	Yes	Yes	10/10
NEUROLOGICAL FEATURES AND MRI ABNORMALITIES											
Intellectual disability	Mild	Mild/mod	Mod	Mild/mod	Sev	Yes (not specified)	Sev	Mod	Yes (not specified)	Yes (not specified)	10/10
Speech delay	Yes	Yes	Yes	Yes	Yes	n.r.	Yes	n.r.	Yes	n.r.	7/7
Epilepsy	No	No	Yes	No	n.r.	Yes	No	n.r.	Yes	No	3/8
Hypotonia	No	Yes	Yes	No	n.r.	Yes	Yes	n.r.	Yes	n.r.	5/7
Behavioral problems	Yes	Yes	No	Yes (hyperactive)	n.r.	n.r.	Yes (sleep disturbance)	n.r.	Yes ASD	n.r.	5/6
MRI results	n.a.	HCC, PG	CA(1), HCC, ELV, MCM, WML	CA(2), HCC, ELV, TP, MCM	n.r.	CA(3), HCC, TP, MCM	HCC, TP, MCM,PG	WML	WML	HC	8/8
Neonatal feeding difficulties	Yes	Yes	Yes	Yes	Yes	No	No	n.r.	No	n.r.	5/8
OTHER ORGANS AND SISTEMS											
CHD	PVS, ASD, VSD	No	NS LVC, IV	No	n.r.	PDA, PFO, BAV	VSD	n.r.	No	No	4/8
Ectodermal anomalies	n.r.	Recurrent facial and body eczematous rashes in childhood; extreme dry skin and itching	n.r.	Eczema	n.r.	n.r.	n.r.	n.r.	Eczema	Ichthyosiform changes, hyperkeratotic papules	4/10
Skeletal anomalies	Scoliosis, small hands and feet	Small hands and feet[b]	Plagiocephaly, scoliosis, hyperlaxity, small hands and feet								3/10
Additional features	Stipsis, renal lithiasis, hydronephrosis	Wide based gate, sensorineural deafness, myopia, chorioretinal atrophy, hypernasal voice, velopharyngeal synechiae	Bilateral SPC	Recurrent pneumonias	Diabetes mellitus	Umbilical hernia, tracheomalacia, cryptorchidism	Mild visual impairment, sensorineural deafness, abnormal creases, stereotypic movements		Recurrent otitis media, stereotypic movements	Congenital cataracts, hydronephrosis, nasolacrimal duct obstruction	

Variants have been submitted to ClinVar (c.475G>A, SCV002605544; c.184G>A, SCV002605545).

ASD autism spectrum disorder, *BAV* bicuspid aortic valve, *CA* cerebellar anomalies described as follows: (1) dysgenetic vermis and right cerebellar hemisphere, (2) hypoplastic cerebellar vermis, (3) abnormal cerebellar foliation, lower vermis hypoplasia, *ELV* enlarged lateral ventricles, *F* female, *HC* hydrocephalus, *HCC* hypoplastic corpus callosum, *IV* insufficiency of all valves, *M* male, *MCM* mega cisterna magna, *mod* moderate, *n.a.* not available, *n.r.* not reported, *sev* severe, *NS LVC* non-synchronic left ventricle contractions, *PDA* patent ductus arteriosus, *PFO* patent foramen ovale, *PG* polymicrogyria/pachygyria, *SPC* single palmar crease, *TP* thin pons/brain stem, *WML* white matter lesions.

[a]For a comprehensive description of facial dysmorphisms see Supplementary Table S3.

[b]Hands/feet measurements were compared to height and age, using standard charts [49]. Parameters were scored under the 5th centile.

and RAC1^{A159V} proteins, while showed a strong reduction of RAC1^{E62K} and RAC1^{G12V} (Fig. 1A). Treatment with the proteasome inhibitor, MG132, recovered levels of RAC1^{E62K}, indicating an accelerated degradation of this mutant by the proteasome machinery (Fig. 1B). Next, we assayed the levels of active, GTP-bound WT and mutant RAC1 by performing pull-down assays on lysates from HEK-293T cells transfected with HA-tagged RAC1 mutants. Similar increased levels of normalized GTP-bound RAC1^{E62K} and RAC1^{A159T} proteins with respect to WT RAC1 were observed, which however were lower than those characterizing the RAC1^{A159V} and RAC1^{G12V} mutants (Fig. 1C). Considering the absolute GTP-bound RAC1 levels of proteins, we observed that RAC1^{E62K} behaved as a weakly constitutively activated GTPase, while RAC1^{A159T} showed a full CA behavior, similar to that characterizing RAC1^{A159V} and RAC1^{G12V} (Fig. 1D). To further confirm the GoF effect of the two *RAC1* variants, we tested their impact on cell morphology. As shown in Fig. 2A, WT RAC1-expressing cells exhibited an irregular, variable shape, with only a few round cells, similarly to what was observed in cells expressing the DN RAC1^{T17N} protein [26]. Conversely, the expression of all the other tested mutants variably promoted cell rounding, with a weaker effect exerted by RAC1^{E62K}, supporting their activating impact. To quantitate these morphological changes, we evaluated the RI of cells (Fig. 2B), documenting a significantly lower RI in mutated cells, with RAC1^{A159T} acting as the most activated between the two mutants (Fig. 2C). Overall, these data validate the GoF behavior of the two disease-causing variants and provide evidence for their differential impact on protein levels and function.

Structural analysis

To further explore the effect of the amino acid changes on protein function, we performed structural modeling analyses. A159 is a highly conserved residue mapping at the nucleotide-binding pocket (Fig. 3A). Specifically, it directly contributes to the stability of nucleotide binding by interacting with the purine ring of GTP/GDP. The alanine-to-threonine substitution at codon 159 is expected to locally alter the conformation of the nucleotide binding pocket and consequently RAC1 affinity for GTP/GDP. Of note, mutations affecting this region in RAS proteins have been proved to exert an activating effect on protein function both in cancer and in RASopathies by promoting the GEF-independent release of GDP [27–29].

E62 is adjacent to Q61, a key residue mediating GTP hydrolysis representing one of the major mutation hotspots in cancer [28, 29], and is involved in multiple polar and electrostatic interactions with residues binding the phosphate group of GTP/GDP (Fig. 3A). It also contributes with interactions that are relevant for the proper conformation of the surface mediating binding to signaling partners, which are predicted to be perturbed upon replacement with the oppositely charged lysine (Fig. 3A). Thus, besides the activating effect, the E62K substitution is expected to have a more complex behavior in which opposite perturbing effects (i.e., disrupted GTP hydrolysis *vs* protein structural rearrangement affecting stability and protein-protein interactions) result in a mildly activated mutant, in line with the experimental findings.

Clinical findings

The natural history and clinical features of both subjects are detailed in Fig. 3B, Table 1, Supplementary Table S3, and Supplementary Clinical Reports.

Subject 1 is a 14-year-old boy with speech disorder and mild ID, multiple congenital heart defects (CHD), and facial dysmorphisms. He presented with hydronephrosis, and right inguinal hernia. Since 12 years old, he showed increasing difficulties in social interaction, worsening of intellectual competences, and behavior anomalies characterized by impulsivity, compulsivity, and anxious component.

Subject 2 is a 27-year-old woman with speech disorder, mild ID, facial dysmorphisms and peculiar behavior. Family history reveals late-onset deafness in her father (20 years), which was treated with hearing aids at 45 years. At 6 years, she was diagnosed with severe neurosensory deafness treated with hearing aids. A brain MRI scan revealed mild posterior corpus callosum hypoplasia and left fronto-insular pachygyria. At our observation (15 years), she presented with behavior anomalies characterized by impulsivity, compulsivity, stubbornness, anxious component, unexplained fears, and panic attacks.

We systematically assessed the clinical and facial features for the ten individuals with pathogenic *RAC1* variants, which are summarized in Table 1 and Supplementary Table S3. A relatively homogenous presentation in the absence of any obvious genotype-phenotype correlation was apparent, except for macrocrania in two individuals carrying pathogenic variants involving the residue V51. Overall, all subjects shared ID with speech delay (10/10 and 7/7, respectively), a wide array of brain abnormalities (8/8) (Table 1 and Supplementary Table S4), behavioral abnormalities (5/6), hypotonia and neonatal/childhood feeding difficulties (5/7 and 5/8, respectively). CHDs were also common (4/8), while epilepsy was reported in 3/8 subjects. We also observed recurrent ectodermal anomalies, mainly represented by eczematous rashes, with or without ichthyosiform manifestations (4/10), and various skeletal anomalies (3/10), such as small hands and feet (3/10). Two individuals presented with congenital sensorineural deafness (subject 2 from the present report and subject E from [7]), and two showed hydronephrosis (subject 1 from the present report and subject K from [15]) (Table 1). We evaluated facial dysmorphisms in all the individuals whose available clinical pictures could be blind reviewed by three experienced clinical geneticists (MP, FCR and DM) (Supplementary Table S3). Common features included a high anterior hairline (9/9), arched eyebrows (8/9) with tendency to lateral sparse (7/9) and mild synophrys (4/9), a prominent nasal bridge (7/9), mild widely spaced eyes (8/9), wave-shaped palpebral fissures (7/9), overhanging columella (6/9) with a bulbous nasal tip (6/9), a short philtrum (7/9), deep nasolabial folds (8/9), thin upper lip (7/9), abnormally spaced teeth with or without diastema of superior incisors (6/6), everted lips (both superior and inferior) (5/9), and a long pointed chin (7/9).

Clinical profiling of *RAC1* and *RAC3*-related disorders

The comparison among main clinical features associated with *RAC1* and *RAC3* variants revealed a common core of signs/symptoms characterized by DD/ID, brain abnormalities, hypotonia, failure to thrive/feeding difficulties, seizures, and behavior anomalies (Supplementary Table S4). Although reported in both cohorts, differences in MRI anomalies and ID were evidenced both in frequencies and severity. Facial dysmorphisms were quite distinctive between the two conditions. Although affected individuals shared high anterior hairline, arched eyebrows with tendency to lateral sparse and mild synophrys, a prominent nasal bridge, and a long pointed chin, *RAC1* mutated subjects presented with wave-shaped palpebral fissures, short philtrum with overhanging columella, and a thin upper lip, while *RAC3* mutated individuals showed upslanted palpebral fissures with short nose and upturned nares [3].

RAC1-3/CDC42 mutation spectrum

Rho GTPase superfamily is characterized by a highly conserved common structure of "G domain" characterized by five α helices, six β strands and five loops, also known as "G boxes", which are the main mediators in GTP/GDP binding. RAC1-3 and CDC42 proteins show high similarity in G boxes consensus sequence, localization, and length: G1 box (P-loop/Walker A) (residues 10–17 in RAC3), G2 box (effector domain/Switch 1) (residues 25–40), G3 box (Walker B motif/Switch II) (residues 57–61), G4 box (residues 115–118), and G5 box (residues 158–160) [3, 30, 31]. However,

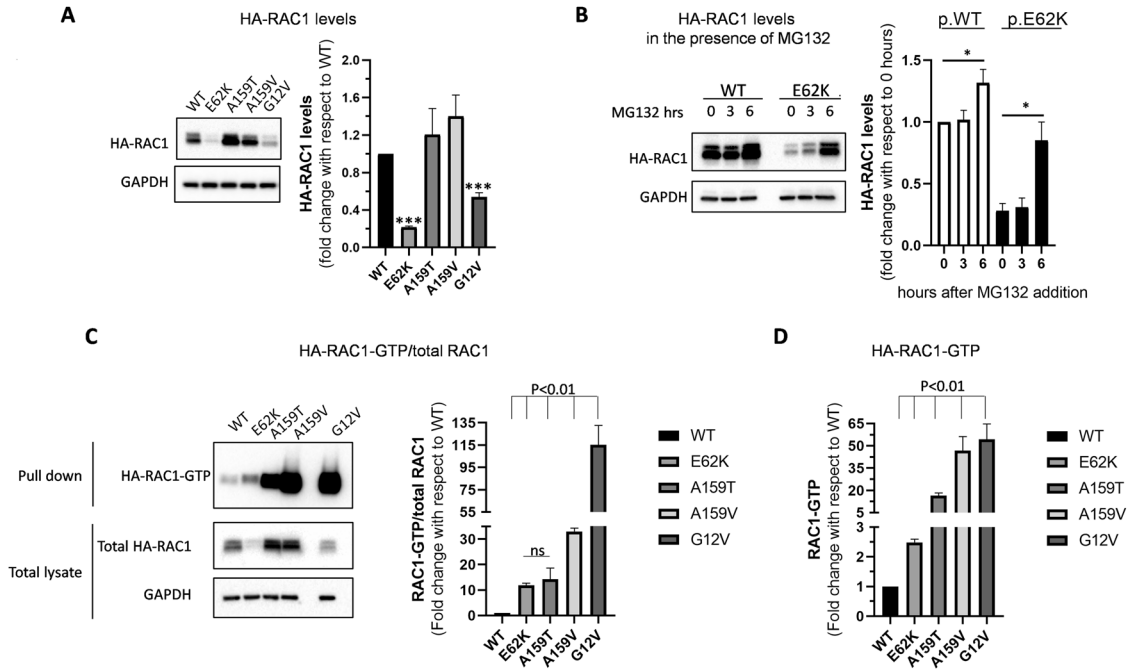

Fig. 1 ***RAC1* mutations variably affect protein stability and GTP binding in COS-1 transfected cells. A** Western blot analysis of exogenous RAC1 levels in COS1 transfected cells. HA-tagged RAC1 fold-level changes are calculated with respect to cells overexpressing the WT protein. Data are presented as a mean fold change ± SEM ($n = 3$). Statistical significance of differences were assessed by *t*-test, corrected for multiple comparisons using Holm-Sidak method (***$p < 0.001$). **B** $RAC1^{E62K}$ undergoes accelerated degradation via the proteasome machinery. HA-tagged $RAC1^{E62K}$ changes are compared with cells overexpressing the WT protein. Data are presented as a mean fold change ± SEM ($n = 3$). Statistical significance of differences was assessed by *t*-test, corrected for multiple comparisons using Holm-Sidak method (*$p < 0.05$). **C**, **D** Representative western blot analysis of proteins after pull-down assay and bar charts of the mean fold change values of three independent experiments. Pull down of the GTP-bound HA-RAC1 from the total protein lysates is performed using a GST-human Pak1-(PBD). Immunoblot analysis of total cell lysates identified the levels of total protein (Total HA-RAC1). GTP-bound HA-tagged RAC1 level-fold changes are calculated with respect to cells overexpressing WT protein. In **C**, GTP-bound RAC1 levels were also normalized with respect to total HA-RAC1 levels. Differences are statistically significant with respect to WT RAC1-expressing cells. Data are presented as a mean fold change ± SEM ($n = 3$). Significance is determined by multiple *t*-test, corrected for multiple comparisons using Holm-Sidak method. GAPDH, glyceraldehyde-3-phosphate dehydrogenase.

slight differences in boundaries of these domains do exist among proteins. We revised all the pathogenic variants in these GTPases (Fig. 4), confirming a previously recognized hotspot in Switch II and highlighting a novel hotspot in Switch I involving highly conserved residues among orthologs and paralogs, located between residues 28–39. Notably, recurring variants at specific residues (E62 and Y64 in G3/Switch II) were reported in all proteins. We also evidenced specific recurring changes in G1 box (G12) and G2/Switch I box (P29 and P34) in RAC2, RAC3 and CDC42, and in G5 box (C157 and A159) in RAC1 and CDC42, respectively.

DISCUSSION

MRD48 is a rare and poorly characterized syndromic NDD caused by dominantly acting variants in *RAC1*, with eight individuals reported so far. Here, we describe two additional subjects with previously unreported activating variants. We review the clinical and facial features of MRD48-affected individuals, identifying a core clinical presentation characterized by DD/ID with speech delay, brain abnormalities, behavior anomalies, hypotonia, neonatal/childhood feeding difficulties, and distinctive facies. Although previous reports failed in recognizing a facial gestalt, we identify recurrent features by systematical review of available pictures. Among them, a high anterior hairline, arched eyebrows with tendency to lateral sparse, wave-shaped palpebral fissures, overhanging columella with a bulbous nasal tip, a short philtrum, deep nasolabial folds, abnormally spaced teeth, with or without diastema of superior incisors, and a long pointed chin may be suggestive for this condition (Supplementary Table S3). Notwithstanding the heterogeneous functional impact of *RAC1* mutations, the clinical phenotype does not appear to correlate with the functional effect of the identified variants with the exception of the association between OFC and variants involving key residues (V51, macrocephaly; C18 and N39, microcephaly). A wider series of affected subjects is needed to confirm these findings.

Rac1 knock-out (KO) mice are embryonic lethal [32]. To overcome this constraint, multiple conditional KO and Knock-in (KI) *Rac1* mouse models have been reported in order to study specific effects of increased or abolished Rac1 activity in brain and other organs development and function (Supplementary Table S5 and Supplementary Text for a comprehensive revision). Many clinical features observed in affected subjects (i.e., microcephaly, ID, neurological signs, behavior anomalies, CHD, and oropharyngeal arches anomalies as those observed in Subject 2, ectodermal abnormalities, and neurosensory deafness) fit well with the malformations/anomalies observed in these models (Supplementary Table S5 and Supplementary Text). Notably, the perturbed development of neural crest cell (NCC)-derived tissues documented in NCC-targeted *Rac1* conditional KO mice may explain both craniofacial and cardiac features recurring in affected individuals (see Supplementary Text) [33–35]. Cardiac NCCs contribute to the formation of the anterior second heart field (SHF) from which the right ventricle, the interventricular septum, the aortic-pulmonary septum, and the outflow tract (OFT) develop, generating the aortic and pulmonary valves and trunks [35]. Of note, 5/10 MRD48 individuals presented with a CHD, mainly valve anomalies and septal defects. SHF-specific KO *Rac1* mice show

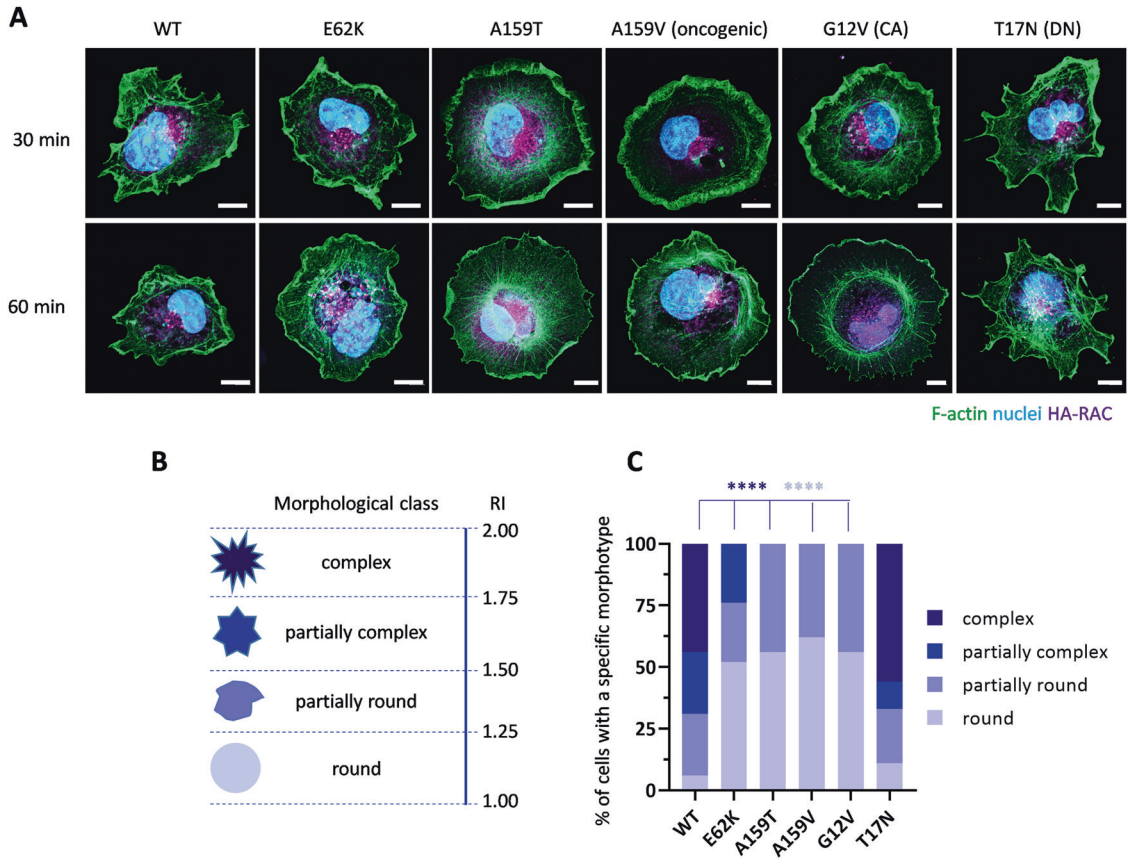

Fig. 2 ***RAC1* mutations affect cytoskeletal rearrangement and cell shape. A** Representative confocal images of COS-1 cells expressing HA-tagged RAC1 WT or mutants cultured for the indicated period on fibronectin matrix and stained to detect HA-RAC1 (magenta), f-actin (green) and nuclei (blue). **B** Schematic representation of cells with respect to their shape and related roundness index (RI): lower values of RI correspond to higher cell roundness. RI was calculated as described in materials and methods and cells were grouped into four different morphological classes (round, $1.0 < RI < 1.25$, partially round, $1.25 < RI < 1.50$, partially complex, $1.50 < RI < 1.75$ and complex, $RI > 1.75$). **C** Incidence of cell morphotypes. Bar graph representing the percentage of cells having different morphologies in HA-tagged RAC1 transfected cells 30 min after seeding on fibronectin matrix, based on the classification described above in **B**. Data are plotted as a percentage of the cells analyzed from the mean of three independent experiments. Two sided Fisher's exact test in 2×2 contingency table is used (WT *vs* each mutant and each cellular type *vs* the other morphologies). Multiplicity adjusted *p*-values are reported. Round and complex morphotypes were extremely significant (****$p < 0.0001$) for all mutants except T17N. E62K, partially round and partially complex, not significant. A159T, A159V and G12V, partially complex, $p < 0.001$; A159T and G12V, partially round, $p = 0.072$; A159V, partially round not significant. T17N, complex, partially round and round, not significant; T17N partially complex $p = 0.016$. $N \geq 20$. Bar = 10 μm.

right ventricular non-compaction and OFT defects. Three out of five subjects with CHD carried combined associations of septal defects (ASD and/or VSD) and OFT anomalies, such as bicuspid aortic valve and pulmonary valve stenosis as observed in subject 1. Finally, we noted a changing phenotype of the facial features with age. Specifically, widely spaced eyes, bulbous nasal tip and prominent nasolabial folds tend to smoothen in adolescents and young adults. A changing phenotype is observed in various developmental disorders and is likely due to the evolution of craniofacial morphology [36].

MRD48 and NEDBAF share many neurological signs (Supplementary Table S4). This is not surprising taking into account the overlapping expression of *RAC1* and *RAC3* in the nervous system [37]. However, specific MRI anomalies (i.e., hypoplasia/aplasia of corpus callosum, brainstem and cerebellar hypo/dysplasia) seem much more frequent in NEDBAF with respect to MRD48; on the other hand, a subset of *RAC1* mutations correlate with microcrania, suggesting that RAC1 likely plays a major role in neurogenesis and/or apoptosis, while RAC3 is primarily involved in neuronal migration [3]. Pathogenic *RAC1* variants exert variable activity ranging from DN to CA [7, 16]. This is not observed in *RAC3* variants, which almost invariably show a CA behavior [3, 6]. This evidence suggests that downstream interactors may be differentially regulated by *RAC1* with respect to *RAC3* in a cell context-dependent manner. Eventually, Rac3 can partially compensate the lack of Rac1 function in late murine developmental stages, while double conditional KO mice are almost lethal [37]. This finding may in part explain the consistent and statistically significant differences in DD/ID in the two conditions; subjects with pathogenic *RAC1* variants show a milder developmental involvement (5/10 with mild to moderate DD/ID) compared to individuals with *RAC3* mutations, who were all diagnosed with severe to profound ID (Supplementary Table S4). CHD and involvement of other systems are quite rare in NEDBAF; this is expected when considering the confined brain expression of *RAC3* with respect to *RAC1*.

The revision of all reported pathogenic variants in RAC1-3 and CDC42 proteins allowed us to further confirm a variation hotspot in Switch II (G3 Box, see RAC1-3/CDC42 mutation spectrum) and highlight a new hotspot in Switch I (G2 Box, see RAC1-3/CDC42 mutation spectrum) approximately spanning from residues 28–39. The Switch I and Switch II regions are crucial domains in RAS/RHO GTPase proteins, as they are directly involved in the conformational changes controlled by their GTP/GDP-bound state [38]. The most critical motifs that governs Mg^{2+} and GTP/GDP binding, reside within Switch I and Switch II regions [39]. Of note, Y32 is

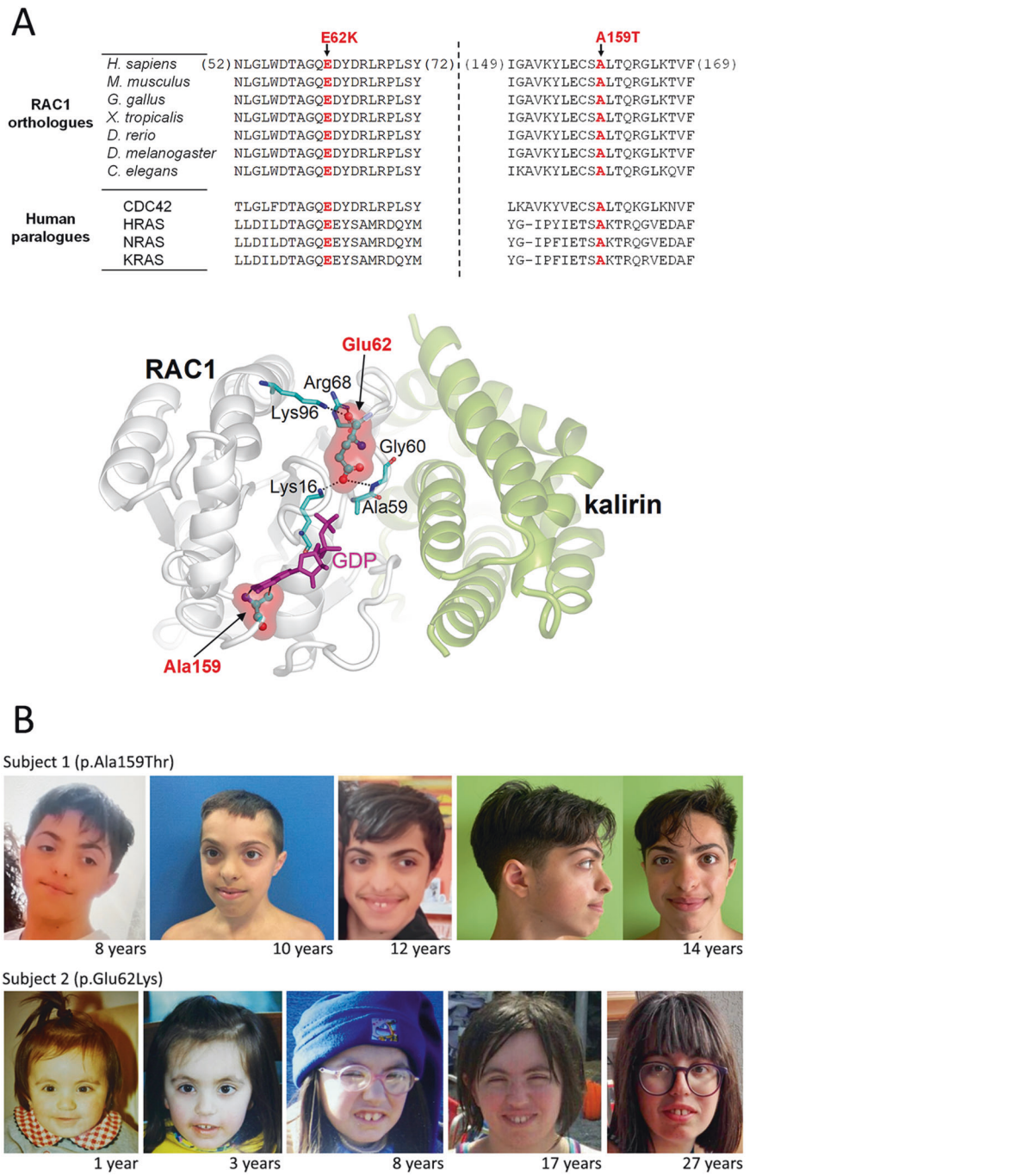

Fig. 3 Structural impact of the pathogenic RAC1 amino acid substitutions and clinical pictures of affected individuals. A Sequence alignment and structure of RAC1. Multiple sequence alignment around residues, Glu62 and Ala159, in homologs and orthologs, and their positions in the crystal structure of human RAC1 complexed with the GEF kalirin DH1 domain (PDB 5O33). Glu62 and Ala159 are shown as sticks and balls with red surface, interacting residues as sticks, and guanosine-5′-diphosphate (GDP) in magenta. Critical interactions by the two residues are indicated by dotted lines. **B** Facial features of Subject 1 (upper line) and Subject 2 (lower line) at different ages. Note the high anterior hairline, arched eyebrows with tendency to lateral sparse (subject 2), mild synophrys, prominent nasal bridge, mild widely spaced eyes, wave-shaped palpebral fissures, overhanging columella, short philtrum, deep nasolabial folds thin upper lip (Subject 2), abnormally spaced teeth, everted lips, and long pointed chin.

mutated in a *RAC1* positive subject [15], P34H is a recurrent variant in both RAC2 and RAC3, and P34Q has been reported as pathogenic substitution in CDC42 [40]. All the critical residues within the DTAGQ motif (Switch II) are variably mutated in RAC proteins (Fig. 4). We evidenced the occurrence of variants at specific residues (i.e., E62 and Y64 in Switch II) in almost all these GTPases. Among them, the recurrent E62K has been observed in all RAC proteins and results to be in frame deleted in RAC3 [3, 7, 12, 13]. The Y64C variant has been described in RAC3 and CDC42, as well; the Y64D substitution has been reported in RAC1 [7]. The Y64C variant has recently been recorded in ClinVar as pathogenic (VCV001333690.1) in a single subject. While this manuscript was under review, a few other individuals with likely pathogenic *RAC1* variants have been reported in ClinVar (W56C,

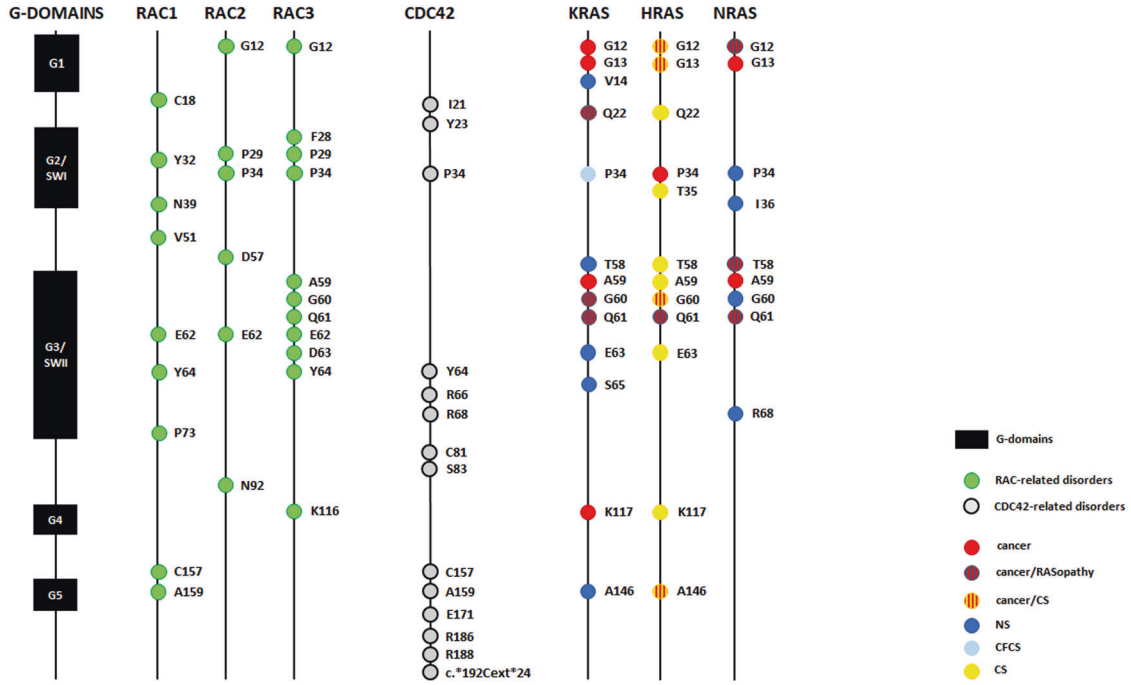

Fig. 4 Mutation spectrum in RAC1 and related GTPases. Affected residues in RAC1-3 proteins (green), CDC42 (gray) and RAS GTPases (representative recurrently mutated in RASopathies and cancer, various colors) are shown together with the major functional motif/domains. Only likely pathogenic/pathogenic variants are reported. Homologous residues are aligned. NS Noonan syndrome, CFCS cardio-facio-cutaneous syndrome, CS Costello syndrome.

VCV001027690.1; R66S, VCV000974895.2; S71F, VCV001685419.1; L165V, VCV001176531.7). While the clinical features and pictures were not available for these subjects, the spectrum of these variants well fits with the mutational diversity and hotspots (Fig. 4). Among the other recurrently mutated residues, G12 is a key residue in RAS superfamily. Amino acid substitutions at codon 12 results in a protein that has impaired GTPase activity and is blocked in its active conformation, and represent common somatic and germline events in cancer and RASopathies, respectively [28, 29, 41, 42]. A159 corresponds to A146 in HRAS, which is mutated in Costello syndrome (MIM 218040) [43, 44]. In general, the spectrum of *RAC1-3* (including the variants reported in the present report) and *CDC42* mutations widely overlaps with those observed in many RASopathies and in cancer.

Overall, our data delineate MRD48 as a clinically variable NDD caused by pathogenic variants in *RAC1* with variegated effects on protein function. Both clinical review and functional evidence suggest a highly heterogeneous set of consequences due to RAC1 dysregulation. The pleiotropic and complex cell type-dependent impacts of the mutant RAC1 proteins possibly explain the differences observed in both MRD48 subjects and "in vitro" models with mirror contrasting results. As evidenced for the E62K RAC1 mutant, potentially different effects (i.e., disrupted GTP hydrolysis, protein structural rearrangement affecting stability and altered protein-protein interactions) may concur to the final functional behavior of each variant, eventually modulating their impact with counteracting consequences on different pathways. A similar behavior has been reported for pathogenic variants occurring in other members of this family of GTPases [3, 17–19]. Altered function of various RAC1 downstream interactors have been associated with NDDs with a wide range of clinical presentation, including PAK1 (MIM 602590) (IDDMSSD, MIM 618158) [45] and TRIO (MIM 601893) (MRD63, MIM 617061; MRD44, MIM 618825) [8]. The RAC1 brain network signaling has also been linked to some syndromic autism spectrum disorder-associated genes, such as *AUTS2* (MIM 607270), *SHANK3* (MIM 606230) and *UBE3A* (MIM 601623) suggesting that the neurobehavioral aspects in MRD48 might be the result of multiple and complex perturbed pathways regulating neuronal subtle cell-to-cell interaction, spine and dendritic formation and synaptogenesis [46–48]. Finally, the overlapping pattern of expression of *RAC1* and *RAC3* in both developing and adult brain, and the evidence of interaction with common downstream effectors further suggest a fine interplay among these two GTPases, which may eventually compensate each other in some functions and may contribute to the wide range of phenotypical presentation observed in both MRD48 and NEDBAF.

DATA AVAILABILITY

The exome sequencing data that support the findings of this work are available on request from the corresponding author (MT). The data are not publicly available due to due to privacy/ethical restrictions. The pathogenic variants identified in this work have been submitted to ClinVar (c.475G>A, SCV002605544; c.184G>A, SCV002605545).

REFERENCES

1. Hall A. Rho family GTPases. Biochem Soc Trans. 2012;40:1378–82. https://doi.org/10.1042/BST20120103.
2. Aspenström P, Fransson A, Saras J. Rho GTPases have diverse effects on the organization of the actin filament system. Biochem J. 2004;377:327–37. https://doi.org/10.1042/BJ20031041.
3. Scala M, Nishikawa M, Ito H, Tabata H, Khan T, Accogli A, et al. Variant-specific changes in RAC3 function disrupt corticogenesis in neurodevelopmental phenotypes. Brain. 2022;145:3308–27. https://doi.org/10.1093/brain/awac106.
4. Porter AP, Papaioannou A, Malliri A. Deregulation of Rho GTPases in cancer. Small GTPases. 2016;7:123–38. https://doi.org/10.1080/21541248.2016.1173767.
5. Stankiewicz TR, Linseman DA. Rho family GTPases: key players in neuronal development, neuronal survival, and neurodegeneration. Front Cell Neurosci. 2014;8:314. https://doi.org/10.3389/fncel.2014.00314.
6. Scala M, Nishikawa M, Nagata KI, Striano P. Pathophysiological mechanisms in neurodevelopmental disorders caused by RacGTPases dysregulation: what's behind Neuro-RACopathies. Cells. 2021;10:3395. https://doi.org/10.3390/cells10123395.

7. Reijnders MRF, Ansor NM, Kousi M, Yue WW, Tan PL, Clarkson K, et al. RAC1 missense mutations in developmental disorders with diverse phenotypes. Am J Hum Genet. 2017;101:466–77. https://doi.org/10.1016/j.ajhg.2017.08.007.
8. Barbosa S, Greville-Heygate S, Bonnet M, Godwin A, Fagotto-Kaufmann C, Kajava AV, et al. Opposite modulation of RAC1 by mutations in TRIO is associated with distinct, domain-specific neurodevelopmental disorders. Am J Hum Genet. 2020;106:338–55. https://doi.org/10.1016/j.ajhg.2020.01.018.
9. Moll J, Sansig G, Fattori E, van der Putten H. The murine rac1 gene: cDNA cloning, tissue distribution and regulated expression of rac1 mRNA by disassembly of actin microfilaments. Oncogene. 1991;6:863–6. PMID: 1905006.
10. Shirsat NV, Pignolo RJ, Kreider BL, Rovera G. A member of the ras gene superfamily is expressed specifically in T, B and myeloid hemopoietic cells. Oncogene. 1990;5:769–72. PMID: 2189110.
11. Malosio ML, Gilardelli D, Paris S, Albertinazzi C, de Curtis I. Differential expression of distinct members of Rho family GTP-binding proteins during neuronal development: identification of Rac1B, a new neural-specific member of the family. J Neurosci. 1997;17:6717–28. https://doi.org/10.1523/JNEUROSCI.17-17-06717.1997.
12. Costain G, Callewaert B, Gabriel H, Tan TY, Walker S, Christodoulou J, et al. De novo missense variants in RAC3 cause a novel neurodevelopmental syndrome. Genet Med. 2019;21:1021–6. https://doi.org/10.1038/s41436-018-0323-y.
13. Lougaris V, Baronio M, Gazzurelli L, Benvenuto A, Plebani A. RAC2 and primary human immune deficiencies. J Leukoc Biol. 2020;108:687–96. https://doi.org/10.1002/JLB.5MR0520-194RR.
14. Lelieveld SH, Reijnders MR, Pfundt R, Yntema HG, Kamsteeg EJ, de Vries P, et al. Meta-analysis of 2,104 trios provides support for 10 new genes for intellectual disability. Nat Neurosci. 2016;19:1194–6. https://doi.org/10.1038/nn.4352.
15. Haugh IM, Pineider JL, Agim NG. Ichthyosiform changes in a patient with RAC1 mutation. Pediatr Dermatol. 2021;38:1590–1. https://doi.org/10.1111/pde.14844.
16. Tian C, Kay Y, Sadybekov A, Rao S, Katritch V, Herring BE. An intellectual disability-related missense mutation in Rac1 prevents LTP induction. Front Mol Neurosci. 2018;11:223 https://doi.org/10.3389/fnmol.2018.00223.
17. Martinelli S, Krumbach OHF, Pantaleoni F, Coppola S, Amin E, Pannone L, et al. Functional dysregulation of CDC42 causes diverse developmental phenotypes. Am J Hum Genet. 2018;102:309–20. https://doi.org/10.1016/j.ajhg.2017.12.015.
18. Lam MT, Coppola S, Krumbach OHF, Prencipe G, Insalaco A, Cifaldi C, et al. A novel disorder involving dyshematopoiesis, inflammation, and HLH due to aberrant CDC42 function. J Exp Med. 2019;216:2778–99. https://doi.org/10.1084/jem.20190147.
19. Coppola S, Insalaco A, Zara E, Di Rocco M, Marafon DP, Spadaro F, et al. Mutations at the C-terminus of CDC42 cause distinct hematopoietic and autoinflammatory disorders. J Allergy Clin Immunol. 2022;150:223–8. https://doi.org/10.1016/j.jaci.2022.01.024.
20. Daimon E, Shibukawa Y, Thanasegaran S, Yamazaki N, Okamoto N. Macrothrombocytopenia of Takenouchi-Kosaki syndrome is ameliorated by CDC42 specific- and lipidation inhibitors in MEG-01 cells. Sci Rep. 2021;11:17990. https://doi.org/10.1038/s41598-021-97478-y.
21. Schneider CA, Rasband WS, Eliceiri KW. NIH Image to ImageJ: 25 years of image analysis. Nat Methods. 2012;9:671–5. https://doi.org/10.1038/nmeth.2089.
22. Richards S, Aziz N, Bale S, Bick D, Das S, Gastier-Foster J, et al. Standards and guidelines for the interpretation of sequence variants: a joint consensus recommendation of the American College of Medical Genetics and Genomics and the Association for Molecular Pathology. Genet Med. 2015;17:405–24. https://doi.org/10.1038/gim.2015.30.
23. Frazer J, Notin P, Dias M, Gomez A, Min JK, Brock K, et al. Disease variant prediction with deep generative models of evolutionary data. Nature. 2021;599:91–95. https://doi.org/10.1038/s41586-021-04043-8.
24. Chang MT, Asthana S, Gao SP, Lee BH, Chapman JS, Kandoth C, et al. Identifying recurrent mutations in cancer reveals widespread lineage diversity and mutational specificity. Nat Biotechnol. 2016;34:155–63. https://doi.org/10.1038/nbt.3391.
25. Majole´e J, Podieh F, Hordijk PL, Kovačević I. The interplay of Rac1 activity, ubiquitination and GDI binding and its consequences for endothelial cell spreading. PLoS One. 2021;16:e0254386. https://doi.org/10.1371/journal.pone.0254386.
26. Ridley AJ, Paterson HF, Johnston CL, Diekmann D, Hall A. The small GTP-binding protein rac regulates growth factor-induced membrane ruffling. Cell. 1992;70:401–10. https://doi.org/10.1016/0092-8674(92)90164-8.
27. Carta C, Pantaleoni F, Bocchinfuso G, Stella L, Vasta I, Sarkozy A, et al. Germline missense mutations affecting KRAS Isoform B are associated with a severe Noonan syndrome phenotype. Am J Hum Genet. 2006;79:129–35. https://doi.org/10.1086/504394.
28. Janakiraman M, Vakiani E, Zeng Z, Pratilas CA, Taylor BS, Chitale D, et al. Genomic and biological characterization of exon 4 KRAS mutations in human cancer. Cancer Res. 2010;70:5901–11. https://doi.org/10.1158/0008-5472.CAN-10-0192.
29. Gremer L, Merbitz-Zahradnik T, Dvorsky R, Cirstea IC, Kratz CP, Zenker M, et al. Germline KRAS mutations cause aberrant biochemical and physical properties leading to developmental disorders. Hum Mutat. 2011;32:33–43. https://doi.org/10.1002/humu.21377.
30. Sanghavi HM, Rashmi R, Dasgupta A, Majumdar S. G-domain prediction across the diversity of G protein families. bioRxiv. 2019;24:888222. https://doi.org/10.1101/2019.12.24.888222.
31. Hiraide T, KabaYasui H, Kato M, Nakashima M, Saitsu H. A de novo variant in RAC3 causes severe global developmental delay and a middle interhemispheric variant of holoprosencephaly. J Hum Genet. 2019;64:1127–32. https://doi.org/10.1038/s10038-019-0656-7.
32. Sugihara K, Nakatsuji N, Nakamura K, Nakao K, Hashimoto R, Otani H, et al. Rac1 is required for the formation of three germ layers during gastrulation. Oncogene. 1998;17:3427–33. https://doi.org/10.1038/sj.onc.1202595.
33. He F, Soriano P. A critical role for PDGFRα signaling in medial nasal process development. PLoS Genet. 2013;9:e1003851. https://doi.org/10.1371/journal.pgen.1003851.
34. Chai Y, Jiang X, Ito Y, Bringas P Jr, Han J, Rowitch DH, et al. Fate of the mammalian cranial neural crest during tooth and mandibular morphogenesis. Development. 2000;127:1671–9. https://doi.org/10.1242/dev.127.8.1671.
35. Leung C, Engineer A, Kim MY, Lu X, Feng Q. Myocardium-specific deletion of Rac1 causes ventricular noncompaction and outflow tract defects. J Cardiovasc Dev Dis. 2021;8:29. https://doi.org/10.3390/jcdd8030029.
36. Allanson JE, Cunniff C, Hoyme HE, McGaughran J, Muenke M, Neri G. Elements of morphology: standard terminology for the head and face. Am J Med Genet A. 2009;149A:6–28. https://doi.org/10.1002/ajmg.a.32612.
37. Pennucci R, Talpo F, Astro V, Montinaro V, Morè L, Cursi M, et al. Loss of either Rac1 or Rac3 GTPase differentially affects the behavior of mutant mice and the development of functional GABAergic networks. Cereb Cortex. 2016;26:873–90. https://doi.org/10.1093/cercor/bhv274.
38. Mosaddeghzadeh N, Ahmadian MR. The RHO family GTPases: mechanisms of regulation and signaling. Cells. 2021;10:1831. https://doi.org/10.3390/cells10071831.
39. Fiegen D, Haeusler LC, Blumenstein L, Herbrand U, Dvorsky R, Vetter IR, et al. Alternative splicing of Rac1 generates Rac1b, a self-activating GTPase. J Biol Chem. 2004;279:4743–9. https://doi.org/10.1074/jbc.M310281200.
40. Asiri A, Alwadaani D, Umair M, Alhamoudi KM, Almuhanna MH, Nasir A, et al. Pancytopenia, recurrent infection, poor wound healing, heterotopia of the brain probably associated with a candidate novel de novo CDC42 gene defect: expanding the molecular and phenotypic spectrum. Genes 2021;12:294. https://doi.org/10.3390/genes12020294.
41. Tartaglia M, Gelb BD. Disorders of dysregulated signal traffic through the RAS-MAPK pathway: phenotypic spectrum and molecular mechanisms. Ann N Y Acad Sci. 2010;1214:99–121. https://doi.org/10.1111/j.1749-6632.2010.05790.x.
42. Niihori T, Aoki Y, Okamoto N, Kurosawa K, Ohashi H, Mizuno S, et al. HRAS mutants identified in Costello syndrome patients can induce cellular senescence: possible implications for the pathogenesis of Costello syndrome. J Hum Genet. 2011;56:707–15. https://doi.org/10.1038/jhg.2011.85.
43. Zampino G, Pantaleoni F, Carta C, Cobellis G, Vasta I, Neri C, et al. Diversity, parental germline origin, and phenotypic spectrum of de novo HRAS missense changes in Costello syndrome. Hum Mutat. 2007;28:265–72. https://doi.org/10.1002/humu.20431.
44. Gripp KW, Lin AE. Costello syndrome: a Ras/mitogen activated protein kinase pathway syndrome (rasopathy) resulting from HRAS germline mutations. Genet Med. 2012;14:285–92. https://doi.org/10.1038/gim.0b013e31822dd91f.
45. Harms FL, Kloth K, Bley A, Denecke J, Santer R, Lessel D, et al. Activating mutations in PAK1, encoding p21-activated kinase 1, cause a neurodevelopmental disorder. Am J Hum Genet. 2018;103:579–91. https://doi.org/10.1016/j.ajhg.2018.09.005.
46. Hori K, Shimaoka K, Hoshino M. *AUTS2* gene: keys to understanding the pathogenesis of neurodevelopmental disorders. Cells. 2021;11:11. https://doi.org/10.3390/cells11010011.
47. Duffney LJ, Wei J, Cheng J, Liu W, Smith KR, Kittler JT, et al. Shank3 deficiency induces NMDA receptor hypofunction via an actin-dependent mechanism. J Neurosci. 2013;33:15767–78. https://doi.org/10.1523/JNEUROSCI.1175-13.2013.
48. Dong T, He J, Wang S, Wang L, Cheng Y, Zhong Y. Inability to activate Rac1-dependent forgetting contributes to behavioral inflexibility in mutants of multiple autism-risk genes. Proc Natl Acad Sci USA. 2016;113:7644–9. https://doi.org/10.1073/pnas.1602152113.
49. Jones KL, Jones MC, and Del Campo M. Smith's recognizable patterns of human malformation. Philadelphia, PA: Elsevier Health Sciences; 2013.

ACKNOWLEDGEMENTS

We are grateful to the families who participated in this study.

AUTHOR CONTRIBUTIONS

MP and MT conceived the work, and wrote the manuscript. AC, CM, FP, VC, LC and MN performed the genomic analyses and analyzed and validated the genomic data. EB performed the structural analyses. MP, FCR, EA, CM and DM collected the clinical data and contributed to the clinical data analyses. EZ, FS, and SC designed and performed the functional analyses. All coauthors helped write and revise the manuscript.

FUNDING

This work was supported by the Italian Ministry of Health (5×1000_2019 and CCR-2017-23669081 to MT, and RF-2018-12366931 and GR-2019-12371203 to FCR), Istituto Superiore di Sanità (Bando Ricerca Indipendente ISS 2020-2022-ISS20-39c812dd2b3c to SC), Fondazione AIRC per la Ricerca sul Cancro (IG 21614, to MT), and Italian Ministry of Research (FOE_2019 to MT).

COMPETING INTERESTS

The authors declare no competing interests.

ETHICAL APPROVAL

The study was approved by the local Institutional Ethical Committee (ref. 1702_OPBG_2018). Clinical data, pictures, DNA samples and other biological specimens were collected, used, and stored after signed informed consents from the participating subjects/families were secured. Permission to publish the clinical pictures and the clinical details was obtained for both individuals.

ADDITIONAL INFORMATION

Supplementary information The online version contains supplementary material available at https://doi.org/10.1038/s41431-023-01351-7.

Correspondence and requests for materials should be addressed to Manuela Priolo or Marco Tartaglia.

Reprints and permission information is available at http://www.nature.com/reprints

Publisher's note Springer Nature remains neutral with regard to jurisdictional claims in published maps and institutional affiliations.

Springer Nature or its licensor (e.g. a society or other partner) holds exclusive rights to this article under a publishing agreement with the author(s) or other rightsholder(s); author self-archiving of the accepted manuscript version of this article is solely governed by the terms of such publishing agreement and applicable law.